Effect of spinal cord injury on neural encoding of spontaneous postural perturbations in the hindlimb sensorimotor cortex

Authors: Jaimie B Dougherty (jaimie.dougherty@drexel.edu)[a], Gregory D Disse (gddisse@ucdavis.edu)[b], Nathaniel R Bridges (nathaniel.bridges@gmail.com) [c], Karen A Moxon (moxon@ucdavis.edu)[a,b]

Affiliations:

[a]School of Biomedical Engineering, Science and Health Systems, Drexel University, Philadelphia, PA 19104 USA

[b]Department of Biomedical Engineering, University of California at Davis, Davis CA 95616 USA

[c] Air Force Research Laboratory Wright Patterson Air Force Base, OH 45433

Author Contribution: JBD, NRB, KAM designed the experiments, JBD and NRB performed the experiments and analyzed the data, JBD, GDD and KAM interpreted the results and wrote the manuscript, GDD prepared the figures.

Running Header: Encoding Posture Responses Post Spinal Cord Injury

Address of Correspondences: Karen A Moxon, Department of Biomedical Engineering, University of California at Davis, One Shields Ave, Davis CA 95616, moxon@ucdavis.edu

Conflict of Interest: none

Acknowledgments: This work was supported by the National Institutes of Health Grant R01 NS096971; National Science Foundation Grant DARE - 1933751; National Center for Advancing Translational Sciences, National Institutes of Health – UL1 TR001860 and linked award TL1 TR001861.

Abstract:

Supraspinal signals play a significant role in compensatory responses to postural perturbations after spinal cord injury (SCI). SCI disrupts descending motor control signals as well as ascending somatosensory information to and from below the lesion. In intact animals, cortical signals are not necessary for basic postural tasks, but neurons in the motor cortex have been shown to respond to periodic postural perturbations. However, the role of the cortex in postural control after spinal cord injury in response to unexpected postural perturbations has not been studied. To better understand how spinal lesions impact cortical encoding of information about unexpected postural perturbations, the activity of single neurons in the rat hindlimb sensorimotor cortex (HLSMC) were recorded during unexpected tilts before and after a complete midthoracic spinal transection. In a subset of animals, limb ground reaction forces were collected as well. Results show that responses in the HLSMC were modulated with changes in tilt severity (i.e. tilt velocity). As velocity of the tilt increased, more information was conveyed by the HLSMC neurons about the perturbation due to increases in both the number of recruited neurons and the magnitude of their response. After SCI hindlimb ground reaction forces were both attenuated and delayed, and the neural responses were delayed and less likely to respond to slower tilts. This resulted an attenuation of the information conveyed by cortical neurons about the tilts, requiring more cells to convey the same amount of information as before the transection. Given that reorganization of the hindlimb sensorimotor cortex in response to therapy after complete mid-thoracic SCI is necessary for behavioral recovery, this sustained encoding of information after SCI could be a substrate for the reorganization that uses sensory information from above the lesion to control trunk muscles that permit weight-supported stepping and postural control.

Keywords: rat, electrophysiology, neural encoding, spinal cord injury, posture

Introduction

Maintaining postural stability is critical for recovery of independent locomotion after spinal cord injury (SCI). Efficient control of posture is equally important for standing and walking (Horak and Macpherson 1996; Orlovsky et al. 1999) as it is for providing support of voluntary limb movements (Massion and Dufosse 1988). Depending on the location and extent of SCI, damage to descending and ascending spinal pathways can result in an impairment of postural control (Horak and Macpherson 1996). The behavioral effect of a complete mid-thoracic lesion of the spinal cord has been well studied (Barbeau et al. 2002; Fung and Macpherson 1999; Macpherson and Fung 1999; Rossignol et al. 1999, 2002). Notably, while postural control is reduced after SCI, brief standing episodes have been reported even after injury in some animal models (Giuliani and Smith 1985; Kellog et al. 1946). Additionally, interventions, including treadmill training (Edgerton et al. 2001, 2004; De Leon et al. 1999; Pratt et al. 1994) and epidural electrical stimulation (Lyalka et al. 2011), have led to modest improvements in this control. Thus, a more thorough understanding of how the entire neural axis encodes for posture before and after SCI can inform therapies that target the restoration of postural control after SCI.

The effects of SCI on limb responses during various postural disturbances have been studied (Chvatal et al. 2013; Lyalka et al. 2005; Macpherson et al. 1997; Macpherson and Fung 1999). Specifically, electromyographic (EMG) recordings in the hindlimbs show increases in response latencies, decreases in response amplitudes, and changes in muscle recruitment strategies after a complete midthoracic transection, suggesting that descending neural circuits from above the lesion are necessary for postural control (Chvatal et al. 2013; Macpherson and Fung 1999). Partial lesion studies in rabbits have suggested that the ventral spinal pathways (reticulospinal and vestibulospinal tracts) arising from the brainstem are critical for postural control whereas dorsal pathways arising from the cortex and midbrain (corticospinal and rubrospinal) are less important (Brustein and Rossignol 1998, 1999; Jiang and Drew 1996; Lyalka et al. 2005, 2009). While these

74 brainstem circuits clearly provide important descending control of posture, cortical responses to
75 periodic (predictable) rotations in the frontal plane (tilts) have also been documented in rabbits
76 and cats, both before (Beloozerova et al. 2003, 2005, 2006; Deliagina et al. 2006) and after SCI
77 (Lyalka et al. 2005, 2009; Musienko et al. 2010). Though cortical activity is not critical for basic
78 postural tasks (Honeycutt and Nichols 2010; Musienko et al. 2008) in intact animals, its role
79 increases substantially after spinal cord injury. It has been shown that cortical reorganization
80 (Ganzer et al. 2013; Manohar et al. 2017) and sprouting of corticospinal axons (Ghosh et al. 2009;
81 Manohar et al. 2017) is associated with recovery of locomotion after injury. More importantly,
82 lesioning the reorganized cortex results in a loss of behavioral improvement achieved after
83 therapy, demonstrating that, in addition to other supraspinal circuits, descending information from
84 the cortex is critical for functional recovery. Therefore, the role of cortical circuits in the encoding
85 of posture and balance is of interest and the impact of spinal cord injury is unknown

86 To better understand the impact of SCI on HLSMC encoding of information about postural
87 perturbations, we assessed the hindlimb ground reaction forces, the responses of ensembles of
88 single neurons in the rat HLSMC, and the interaction of the two during an unpredictable tilting
89 task both before and after a complete mid-thoracic spinal cord transection. In intact animals, when
90 sensory input from the hindlimbs is removed, the response of neurons in the hindlimb
91 sensorimotor cortex (HLSMC) to predictable tilts is greatly attenuated (Karayannidou et al. 2008).
92 This would suggest that cortical responses would also be attenuated after complete spinal
93 transection, resulting in a decrease in the encoding of information about the tilt. Alternatively, it is
94 possible that HLSMC reorganization after SCI allows for continued encoding of unpredictable tilts
95 due to inputs from sensory afferents above the level of the lesion. As reported previously, we
96 observed cortical response modulation to different tilt types in intact rats. Cortical neurons
97 encoded information about the initial velocity of the perturbation within 50ms of the start of tilt,
98 and that the timing and magnitude of the hindlimb ground reaction forces scale with initial tilt

velocity. After a complete spinal transection (PostTx), cortical activity was sufficient to determine if a tilt occurred and to provide information about the initial velocity of the tilt. Despite a reduction, this sustained cortical encoding about postural perturbations even after a complete spinal cord transection could inform therapies that target cortical reorganization. Additionally, since open-loop spinal stimulation has been shown to improve functional outcome after SCI (Harkema et al. 2011; Lavrov et al. 2008; Musienko et al. 2010; Shah et al. 2016), how this cortical information could be used to control a spinal prosthetic is discussed.

Material and Methods

Ethical Approval: All experiments were performed under approval of the Drexel University Institutional Animal Care and Use Committee, followed established National Institutes of Health guidelines (Protocol 19786), and was conducted in accordance with the Animal Research: Reporting of In Vivo Experiments (ARRIVE) guidelines (Kilkenny et al. 2010).

Surgical Procedures

Cortical Implant: 8 Long Evans rats were trained to tolerate a harness and were acclimated to the task for 1-2 weeks. Once adapted to the harness and standing, animals were chronically implanted bilaterally with 16 channel (4x4) Teflon-insulated stainless steel microwire arrays (MicroProbes for Life Sciences, USA) in layer V of the hindlimb/trunk sensorimotor cortex (Figure 1A) using methods standard in our lab (Knudsen et al. 2012; Manohar et al. 2012). Of note, there is an almost complete overlap of hindlimb sensory and motor cortices in the rat (Leergaard et al. 2004). As the electrode was lowered, neural activity was pre-amplified, bandpass filtered between 100Hz and 8kHz and digitized with data acquisition hardware (National Instruments, Austin, TX). Digitized raw signal and waveforms were displayed on a computer with Recorder software (Plexon Inc, Dallas, TX), and also monitored on an oscilloscope and made audible through speakers. The array was lowered in 20 μm increments, no faster than 60 μm/min. At each 20 μm

step, sensory responsiveness was assessed by tapping a blunt tip probe over cutaneous surfaces. Neurons predominately responding to hindlimb stimulation ensured proper electrode position in the hindlimb sensorimotor cortex (Moxon et al. 2008; Nandakumar et al. 2020). Once characteristically large amplitude layer V neurons were visualized on a majority of the channels (at a depth of 1.3-1.6mm), the array was cemented in place. All surgical procedures were performed under general anesthesia (2-3% isoflurane in O_2) via orotracheal intubation. Pain was managed using Buprenorphine SR™ LAB (0.5 mg/kg; Wildlife Pharmaceuticals Inc., USA), and animals were given at least a week to recover from the surgery.

Spinal transection: After intact (PreTx) recordings were complete, animals underwent a complete spinal transection procedure at T8, identical to the methods in previous studies (Knudsen et al. 2012; Manohar et al. 2012). In brief, animals were given prophylactic antibiotics (Baytril 5mg/kg) and were anesthetized with an induction dose of 4% isoflurane followed by maintenance at 1.5-2% isoflurane. A laminectomy was performed at T8/T9. Microdissecting scissors were used to remove the dura, and the cord was transected with iridectomy scissors immediately followed by aspiration. Two surgeons confirmed the lesion visually under 20X magnification. The muscle and skin were sutured in layers with 4-0 non-dissolving suture. Animals were treated with an analgesic (buprenorphine 0.05mg/kg), given 10ml saline, and placed on a heating pad until recovery. After transection, animals were kept on a heating pad and received ongoing care including bladder expression 2-3 times daily, antibiotics, and fluids as needed. Transected animals were given one week of recovery before PostTx recordings were performed. All PostTx recordings were collected within 3 weeks of the injury.

Behavioral Tasks

Tilt Task: The tilt task is shown in Figure 1B. Rats stood in a neutral position on a platform consisting of three Plasti Dip ® (Plasti Dip International, USA) coated plexiglass plates (one for

each hindlimb and for the forelimbs collectively) coupled to a high-performance brushless AC servo motor (J0400-301-4-000, Applied Motion Products, USA). The animal wore a pelvic harness attached to a body weight support system at the pelvis. No vertical weight support was provided PreTx, allowing the animal to freely adjust posture, make small steps, and shift body weight. PostTx, approximately 50% of the weight was supported vertically at the pelvis.

The platform rotated in the frontal plane, remained at the peak angle for approximately one second, then returned to the neutral position while the neural response to the perturbation was recorded. The platform remained in a neutral position for a random inter-trial interval of 2-3 seconds. Tilt type was randomized within a recording session using LabVIEW (2015, National Instruments, USA), and direction was reversed during a subsequent recording session. Several tilt types were programmed using Si Programmer™ (v. 2.7.22, Applied Motion Products, USA) on a digital motor drive (SV7-SI-AE, Applied Motion Products, USA). Start of tilt was defined as the time at which the platform started to move.

Tilt Types: Eight tilt types were classified based on their duration, final tilt angle, and peak velocity. A set of four “constant duration tilts” varied in peak velocity and final tilt angle while maintaining the same duration from tilt onset to maximum angle (Figure 1Ci). In addition, two “constant angle tilts” modified the peak velocity and duration of the tilt, but they reached the same maximum angle (Figure 1Cii). Finally, two “constant velocity tilts” modified the final angle and duration of the tilt with the same peak velocity (Figure 1Ciii). For five of the animals, all tilt types were recorded in the same session with the same population of neurons. For a subset of three animals, only the two “constant final angle tilts” were recorded.

Ground Reaction Forces: Ground reaction forces were measured for the subset of three animals. OEM style single point load cells (LCAE-600 G; Omega, USA) positioned underneath the platform plexiglass plates quantified hindlimb and forelimb ground reaction forces (GRFs). Data was

acquired using LabVIEW software (1000 samples/s), which was filtered offline using a 2nd order Butterworth zero-phase low-pass filter. Sensor data was normalized to a period found in the 200 ms time window prior to the start of each tilt. Positive values indicate additional loading onto the sensor.

Single Neuron Recordings

Populations of single units were recorded simultaneously during the tilting task using methods standard in our lab (Knudsen et al. 2012; Manohar et al. 2012). In brief, prior to every session, neurons were sorted online (Sort Client, Plexon Inc., USA). First, the neural activity was played over speakers to identify if neurons were present. An oscilloscope was used to confirm neural activity. The oscilloscope, waveforms, and the first two principal components were used to sort the cells (typically 1-2 per channel, occasionally 3). A Multichannel Acquisition Processor (MAP, Plexon Inc, Dallas, TX) was used to record from multiple single neurons during each recording session and to record event timestamps. Offline, neurons were categorized as single units if less than 0.5% of spiking occurred in the first 1ms of the inter-spike interval histogram (Offline Sorter, Plexon Inc., USA). All other units were discarded. Waveforms were checked for consistency over the course of the experiment.

To determine cell responsiveness, peristimulus time histograms (PSTHs) were built around the start of tilt (+/- 300 ms) with a 2ms bin in a manner similar to our previous work (Kao et al. 2011; Manohar et al. 2012). Background activity was defined in the 300 milliseconds prior to the start of tilt when the platform had been in the neutral position for a minimum of 1 second. Threshold was defined as the average background activity plus 1.65 times the standard deviation. If five bins (10ms), with no more than 10ms separating them, crossed the threshold, then response was compared to an equivalent background window. If they were significantly different (paired t-test, $p<0.05$), the cell was classified as responsive, and the characteristics of the response were found.

Data Analysis

Ground Reaction Forces: For 3 animals, differences in GRFs were compared between fast and slow tilts and between injury states using a two-way analysis of variance. Peak forces generated during the tilt were averaged for different tilt types before and after SCI.

Neuron Response Profiles: The number of responsive neurons and the response characteristics of those neurons were evaluated between each tilt type and before and after spinal cord injury using two-way analysis of variance or t-tests as appropriate. Using the PSTHs, response characteristics were defined by both the timing and magnitude of the response. The first and last bins to cross threshold were defined as the *first and last bin latencies*, respectively. *Response duration* was the difference between the last and first bin latencies. *Response magnitude* was defined as the sum of the spikes in all the bins between the first and last bin latencies, divided by the total number of trials after subtracting the average background activity.. *Response firing rate* (in Hz) was therefore the response magnitude divided by the duration of the response in seconds. If a neuron responded to multiple tilt types, only the case with the largest response magnitude was used such that each neuron only contributed one observation to analyses.

Neuron Classification**:** For the four constant-duration tilts (Figure 1Ci), neurons were classified based on the number of tilts which elicited a significant response. A “selective” neuron responded to a single tilt type only, a “non-selective” neuron responded to more than one but less than four tilts, and a “scaled” neuron responded to all four tilt types.

Relating Ground Reaction Forces to Neural Responses: To summarize the effect of SCI, changes in the average firing rate of neurons during a tilt were correlated to the change in GRF during the tilt. The data were normalized to the start of tilt and the change in firing rate was plotted against the change in GRF for different tilt types and injury conditions in the clockwise and counterclockwise direction (see Figure 5).

Information Analysis: Information was quantified using a PSTH-based method (Foffani and Moxon 2004). In short, PSTHs were generated to find the average response profile (100 trials) of each neuron to each event. In a leave-on-out manner, individual trials were compared to the average response (generated without the single trial) and the difference between the single trial and the average profiles was calculated in a bin-bin comparison (see Figure 1D). The single trial was classified as either a particular tilt response or a background response by identifying the profile with the smallest difference from the single trial. Performance was expressed as the percentage of correctly classified trials. The information was calculated using Shannon's information formula, formally defined as:

$$I(s;r) = \sum_{s,r} P(r,s) \log_2 \left[\frac{P(r,s)}{P(r)P(s)}\right] \text{ (Equation 1)}$$

Where P(r), P(s), and P(r,s) correspond to the probability of the tilt-perturbation response *r*, the tilt perturbation stimulus *s*, and their joint probability, respectively. *I(s;r)*, which is measured in bits, was calculated for each neuron using the actual and predicted tilt type confusion matrix generated when applying the classifier. Residual bias for *I(s;r)* was then estimated using a bootstrapping procedure by pairing the trial response and tilt types in a randomized order – effectively eliminating their associations. This bootstrapping procedure was performed 20 times, and the calculated bias was subtracted from *I(s;r)* such that 0 bits is chance.

To establish the bin size that resulted in the maximal PSTH classifier performance, a range of bin sizes between 2 and 280ms were considered. The optimal bin size was determined to be 20ms across animals, consistent with our previous work (Bridges et al. 2018), so this bin size was used for all information analyses.

Tilt Detection: Trials from tilt profiles in which the severity of the perturbation (changing velocity and peak angle but keeping duration constant, Figure 1Ci) were used for detection and discrimination analyses. To determine if neurons could detect any tilt severity from standing in a

neutral position, responses of neurons to each of the four constant duration tilts (Figure 1Ci) were compared to their firing rates at stance (baseline) and thus single trials were classified as either a tilt or baseline. To account for differing neurons numbers between animals and conditions, information was calculated twenty times with a random sampling of 34 neurons. This number was chosen since it represented the total number of neurons for the animal with the least number of discernable neurons. The effects of tilt severity and injury on information were compared using a two-way analysis of variance.

Tilt Discrimination: An important feature of proper postural control is the ability to discriminate different perturbation types. For tilt discrimination analyses, single trials were classified as being from one of the four tilt profiles. As with tilt detection analyses, information and performance were calculated from the averages obtained from twenty iterations using 34 randomly selected neurons.

To further explore the encoding for discrimination, the following analyses were performed. First, a set number of randomly selected neurons (from 4 to 34 neurons) was used to determine how population size affected information (neuron dropping). To determine how quickly information was conveyed to the hindlimb sensorimotor cortex, information was calculated with an incremental increase in the event window, from the first 20ms after tilt onset to 280ms after tilt onset. For both analysis types, information and performance were calculated 20 times using a different sampling of neurons.

For information and neuron analysis, 5 animals were tested PreTx condition with 2 sessions each for a total of 10 recordings. 4 of those animals were then evaluated similarly PostTx for a total of 8 recordings. For ground reaction force analysis, 3 animals were tested PreTx and PostTx. All reported values are mean ± standard error.

RESULTS

Ground reaction force magnitude and timing scale with tilt severity and injury

To assess the impact of SCI on the response of the hindlimbs to unexpected tilts in the lateral plane, ground reaction forces (GRF) in response to each hindlimb and to both forelimbs together were collected during the two tilts of constant final angle (varying duration and peak velocity; refer to Figure 1Cii constant angle tilts) before and after the SCI (Figure 2A). As described in previous work (Bridges et al. 2018), before SCI, counterclockwise tilts in healthy animals begin with the platform pushing into the right hindlimb and away from the left hindlimb in the first 100ms, leading to an unloading of force from the left hindlimb sensor. The next 100ms is characterized by an active correction of the animal's center of mass, during which the animal extends the left hindlimb and flexes the right hindlimb in order to shift the center of mass over the base of support. This causes a subsequent increase in the ground reaction forces measured in the left hindlimb sensor. The converse is true for clockwise tilts (data not shown). As expected, the measured GRF of the combined forelimbs is much less than that observed in a single hindlimb since the shifting of the weight is conserved. Nonetheless, the weight on the forelimbs, as measured by the GRF, is unloaded as the tilt is initiated, resulting in an overall reduction in total GRF at the peak of the tilt, suggesting a shift of the center of mass to the hindlimbs.

After SCI, the initial response to the tilt, as the platform moves away from the paw, is similar to the response PreTX. As the platform moves away from the paw, the GRF is reduced. Presumably, spinal circuits below the level of the lesion contribute to a reflex response where the limb is extended resulting in a restoration of GRF. However, unlike in the PreTx response, the GRF in the PostTx condition simply returns to the same force seen at stance, such that the extended position of the paw does not exert any force greater than what was exerted in the neutral position as a harness provided additional support and some of this weight shifted to the forepaw.

To quantify these differences, the forces generated by the hindlimb at the start and end of the faster tilts were compared to those for slower tilts before and after injury. As expected, the initial force was significant greater for faster tilts (effect of tilt type: $F(1,390) = 113.6$, $p < 0.0001$) and this force was reduced after injury (effect of injury: $F(1,390) = 160.6$, $p < 0.0001$) regardless of the tilt type (Figure 2B). However, the difference in force between tilt types was attenuated after SCI (interaction: $F(1,390) = 23.87$, $p < 0.0001$). Furthermore, regardless of injury status, rats initiated a correction of their center of mass more quickly during faster tilts (effect of tilt type: $F(1,392) = 142.2$, $p < 0.0001$; interaction $F(1,392) = 0.41$, $p = 0.53$) but these corrections were significantly delayed after injury (effect of injury: $F(1,392) = 272.2$, $p < 0.0001$) (Figure 2C).

Thus, to stabilize the center of mass within the first 200ms of the onset of the tilt, the response of the hindlimbs to faster tilts was quicker and more robust than those to slower tilts while the response after SCI was delayed and attenuated regardless of tilt type. To assess the impact of tilt type and injury on the final postural adjustment, the forces applied at the maximum angle of the tilt was compared (Figure 2D).

As expected, since the final angle was the same, there was no effect of tilt type on the final force generated by the hindlimbs ($F(1,392) = 0.71$, $p = 0.40$), but there was a significant attenuation of this force with injury ($F(1,392) = 115.7$, $p < 0.0001$). Thus, despite differences in the magnitude and timing of the initial force applied during the tilts PreTx, the animal ultimately applies the same force at the maximum angle of the tilt. After injury, these relationships remain, but the force is attenuated. In an effort to stabilize their center of mass, some of this force is transferred to the forelimbs [Figure 2E; effect of tilt type ($F(1,338) = 10.81$, $p = 0.001$; effect of injury ($F(1,338) = 14.83$, $p = 0.0001$; interaction ($F(1,338) = 0.12$, $p = 0.12$)], while the remainder is taken up by the harness. Thus, after spinal cord injury, the center of mass of the animal shifts forward as more weight is on the forelimbs at the peak of the tilt.

An increasing number of neurons respond to tilts of increasing severity

Neuronal responses to a larger set of tilt types were evaluated to assess the impact of SCI on the encoding of the postural shifts noted above. Populations of single neurons were recorded while animals were subjected to eight different rotations in the frontal plane at random intervals. These tilts maintained either constant duration, constant final angle, or constant peak velocity (Figure 1C). For neurons with a significant response to at least one tilt type, their response profiles (response magnitude, duration of response, latency of response) were compared across tilt types and between Pre and PostTx. The number of cells that responded, or responsive neurons, were different depending on the tilt type ($F(7,63) = 22.00$, $p < 0.0001$). This change in responsive neurons was observed if the peak velocity was changed but not if the peak velocity was held constant (Figure 3A). Thus, more neurons were recruited into the response primarily when the severity of the tilt was increased.

After complete spinal transection (PostTx), there was a trend toward an overall reduction in responsive neurons ($F(1,9) = 4.986$, $p = 0.0524$). This was observed despite an unchanged number of discriminable neurons PostTx (Paired t-test, $t(3) = 1.140$, $p = 0.34$). However, just as in the PreTx condition, neuron recruitment remained tuned to tilt severity (changes in peak velocity).

Duration of neuronal responses also increased with increasing severity of tilt

The magnitude of the response was similarly modulated by tilt type ($F(7,1524) = 0.014$, $p = 0.0142$) with increasing spikes per tilt with increasing severity but no change in number of spikes when severity was held constant. Interestingly, there was no effect of injury on the magnitude of the response, suggesting that information about the tilt is reaching the brain despite the injury ($F(1,1524) = 0.394$, $p = 0.536$). However, for both Pre- and PostTx conditions, the change in response magnitude for more severe tilts was not due to changes in firing rates ($F(7,1524 = 0.81$),

338 p = 0.815; Figure 3B) but rather to increases in response durations ($F(7,1524) = 0.749$, $p = 0.0009$;
339 Figure 3C). Therefore, increases in the severity of the tilt resulted in an increase in the duration
340 of the response both pre and post SCI, regardless of the duration of the tilt.

341 **Responses to tilts are delayed, but not attenuated, after transection**

342 Interestingly, response latencies were dependent on the severity of the tilt, similar to the duration
343 of the response (Figure 3D). Furthermore, despite SCI having no impact on the firing rate or
344 magnitude and duration of response, injury delayed the timing of the response (Figure 3D). In
345 fact, after injury, the response onset, was significantly delayed by about 10 milliseconds (first bin
346 latency: PreTx: 54.1 ± 62.3 ms and PostTx: 63.7 ± 67.1ms, $F(1,1524) = 11.22$, $p = 0.0008$).

347 In summary, as the severity of the tilt increased, the number of responding neurons and duration
348 of the response increased while the latency of the response shifts earlier without a change in firing
349 rate. These findings emphasize the importance of the severity of the tilt on the neural response.
350 Post SCI, the severity of tilt had similar impact on the neural response, but the response was
351 shifted later without impact on the magnitude of the response. Therefore, in an unexpected
352 postural perturbation, neurons in the hindlimb sensorimotor cortex respond to the severity of the
353 tilt even in the absence of sensory feedback from the hindlimbs. The shift in latency after SCI
354 suggests this response in the hindlimbs is due to sensory information about the tilt coming from
355 the upper trunk and forelimbs.

356 **Some neurons scale their responses to tilts of increasing severity**

357 To further explore the responsiveness of neurons to tilts of increasing severity (peak velocity),
358 neurons were classified into three classes depending on the range of tilts they responded to (out
359 of four possible tilts): (1) Selective, neurons responsive to only one tilt type; (2) Nonselective,
360 neurons responsive to two to three tilt types; or (3) Scaled, responsive to all four tilts (examples
361 seen in Figures 4A-C, respectively).

In addition to delayed response to tilt after transection, there was a shift in the classification of neurons (Figure 4D), with a decrease in the proportion of scaled neurons (39.6% to 17.0%), an increase in the proportion of selective neurons (21.4% to 39.7%), and a modest increase in non-selective neurons (39.1% to 43.3%) ($\chi^2(2) = 16.06$, $p = 0.0003$). This shift occurred due to a reduced response to the least severe tilts PostTx. In fact, when classifying the selective neurons by the tilt to which they responded (Figure 4E), there was a significant change in these proportions ($\chi^2(3) = 12.69$, $p = 0.0054$), with the biggest change being a reduction in the number of cells uniquely responsive to the lowest-severity tilt (33% v. 13%). Thus, this reduction in scaled neurons is likely due to the fact that neurons previously responsive to all tilts may no longer respond to the mildest tilts after injury, leading to a classification as either a selective (responding to one tilt type) or non-selective (responding to 2-3 tilt types) neuron.

Impact of SCI on neuronal dynamics during tilt

To visualize the impact of SCI on the change in firing rate of the population of neurons during tilt, the average response of neurons during each tilt was plotted against the change in GRF. Examining the left hindlimb during clockwise and counterclockwise tilts, the GRF changes first, before the increase in average firing rate (Figure 5A). Then, the firing rate peaks at about the same time as the peak unloading of the limb due to the movement of the platform. As the limb begins to exert a restorative force to stabilize the animal's center of mass, the firing rate of the population starts to decline but does not quite return to baseline before the GRF reaches its maximum restorative force. For less severe tilts, this trajectory pattern is simply scaled down. As the population of cells are the same for the clockwise and counterclockwise tilts, these data suggest that in each hemisphere, a subset of cells are responding to the contralateral limb's extension while others are responding to the contralateral limb's flexion. After injury, the loading, unloading, and final restorative forces are attenuated, likely due to the harness support and the

shift of weight to the forelimbs, and the neuronal firing rate is also reduced (Figure 5B), resulting in a similar shaped trajectory, albeit reduced in size.

Neurons encode for the detection of tilt

Since neurons respond to the tilt even after a complete spinal transection and changes in the severity of the tilt (peak velocity) are the greatest drivers of that response, we wanted to gain insight into how these neurons encode information about the tilt. Specifically, we investigated how neurons encode for the occurrence of a tilt (i.e. is the platform stationary or has it tilted?) and the magnitude of the severity of the tilt (i.e. what was the peak velocity?) as well as the effect, if any, of SCI on that encoding. The first step to evaluate the encoding of tilt was to quantify the information that a tilt occurred (tilt detection) using a fixed number of neurons (Figure 6A).

As expected from the increase in the number of responsive neurons and the increase in the magnitude of their response with increasing severity, the information that a tilt occurred within the HLSMC increased with the severity of the tilt both PreTx (0.27 for least severe to 0.60 bits for most severe), and PostTx (0.14 bits for least severe to 0.39 bits for most severe tilts; $F(3,64)=18.93$, $p < 0.0001$). After transection, the information about tilt detection was significantly reduced [$F(1,64) = 31.03$, $p < 0.0001$, interaction ($F(3,64) = 0.42$, $p = 0.7406$]. Since the number of neurons used to compare PostTx to PreTx was the same, this reduction in information is unlikely to be due exclusively to the trend toward fewer responsive neurons PostTx.

Neurons convey considerable information about tilt type both Pre- and PostTx

Though the detection that a tilt occurred is the first step in understanding how neurons encode for postural responses, of greater interest is discriminating between different types of tilts as the severity of the tilt increased, which would suggest the information necessary to determine the postural adjustments that need to be made to maintain balance. As expected, the ability of

populations of neurons to discriminate between tilt type was dependent on both the number of neurons used (Figure 6Bi $F(12,208) = 8.22$, $p < 0.0001$) and the amount of time that passed from tilt onset (Figure 6C; $F(13,224) = 7.56$, $p < 0.0001$). For the same sized population, a significant reduction in information was observed after transection compared to before (Neuron Dropping: $F(1,208) = 19.56$, $p < 0.0001$; Window Size: $F(1, 224) = 27.60$, $p < 0.0001$). When comparing the number of neurons used (Figure 6B), as few as twelve neurons were able to convey at least 0.2 bits of information about tilt detection in the PreTx condition. PostTx, twenty neurons were needed to convey comparable levels of information, likely arising from the decreases in cells with responses to less severe tilts after spinal cord transection. Thus, the nervous system can compensate for the loss in information about postural perturbations by recruiting more neurons into the task after SCI. As expected, as the window of time after the tilt onset used to calculate the information increased (Figure 6B), information about tilt discrimination increased. PreTx, the population of neurons conveyed a considerable amount of information (more than 0.2 bits) about the tilt type within the first 60 milliseconds of the tilt. After injury, an additional 60 milliseconds were needed (120ms) after tilt onset to reach similar information levels, consistent with the delayed neuronal responses seen PostTx. Information continued to increase over time for both PreTx and PostTx conditions, with information reaching 0.40 bits PreTx and 0.29 bits PostTx within 300 ms.

Therefore, as with tilt detection, both the reduction in the number of responding neurons PostTx and differences in the firing patterns of neurons contribute to the loss of information about the discrimination between different types of tilts after SCI.

Discussion

Although weight-bearing and stereotypic locomotor movements can be restored following a complete spinal injury through activation of spinal circuits below the lesion (Antri et al. 2002; Barbeau and Rossignol 1990; Van Den Brand et al. 2012; Harkema et al. 2011; Ichiyama et al. 2005; Lavrov et al. 2006; Sławińska et al. 2012), there is a need to ensure adequate postural stability (Bridges et al. 2018; Ganzer et al. 2016; Kao et al. 2011; Rath et al. 2018). An understanding of how the brain encodes for this stabilization before and after spinal cord injury could be used for the design of therapeutic interventions that aim to enhance postural responses and decrease the morbidity and mortality associated with fall incidence. The data presented here suggest that the hindlimb sensorimotor cortex (HLSMC) encodes information about the severity of an unexpected perturbation by changing the number of responsive neurons and altering the duration, but not firing rate, of their responses. Moreover, after a mid-thoracic spinal cord transection, which prevents sensory information from the hindlimbs reaching supraspinal levels, information about the tilt continues to be encoded in the HLSMC with similar, albeit delayed, neural response dynamics.

Role of Afferent Feedback and Effects of Spinal Cord Injury on the Encoding of Postural Responses in Unexpected Perturbations

The work presented here, in which animals were subjected to perturbations that were unexpected in timing and severity both before and after spinal cord injury can be compared to previous studies on behavioral and neuronal responses to predictable tilts in the frontal plane (Beloozerova et al. 2005, 2006). In the previous studies using intact rabbits or cats, the animals compensate for the tilt by extending the limb when the platform moves down and flexing the limb when it moves up. While we recorded ground reaction forces (GRFs) and not limb kinematics or trunk movements from a subset of animals, our animals behaved similarly to shift their center of mass over their base of support, maintaining an upright position and preventing falling. The use of kinematics in future studies will allow for a better assessment of post-transection behavior, as weight-supporting

459 harnesses undoubtedly affected the ground reaction forces after SCI. With respect to neural
460 responses, we observed unique responses in the HLSMC to unexpected tilts, just as cortical
461 modulation was previously observed in response to tilts in both rabbits (Beloozerova et al. 2006)
462 and cats (Beloozerova et al. 2005).

463 Despite these similarities, there are key differences that distinguish our work. First, in cats
464 (Beloozerova et al. 2005), the activity of pyramidal tract neurons in the hindlimb motor cortex was
465 almost exclusively correlated with extension of the contralateral limb. In the present study, when
466 the tilt was unexpected, cells responded to both extension and flexion, suggesting a more robust
467 response to unexpected tilts. Second, the peak firing rate in response to unexpected tilts for intact
468 rats was over 30 Hz, about double the rate of those previously reported (Beloozerova et al. 2005).
469 This would suggest that unexpected perturbations create greater cortical responses. This is
470 consistent with EEG and TMS studies in humans showing that the magnitudes of evoked cortical
471 responses and postural muscle activations are greater during expected compared to expected
472 postural perturbations (Adkins et al. 2006; Dietz et al. 1985, 1989; Fujio et al. 2018; Jacobs et al.
473 2008).

474 Third, we observed a sustained cortical response to tilts even after removal of hindlimb afferents.
475 This is in contrast with previous work that showed that suspending a hindlimb during platform tilts
476 (and thus removing its sensory inputs) led to a strong attenuation of the response in the
477 contralateral hindlimb motor cortex (Karayannidou et al. 2008). In the current study, however, a
478 complete mid-thoracic spinal transection that removed all sensory input from below the lesion
479 simply caused a delayed neural response to unpredictable tilts in the HLSMC, but had no effect
480 on the magnitude of the response. The unexpected tilts in this work better reflect instantaneous
481 loss of balance and provide insight into the role of the cortex during a more complex balance task.
482 Furthermore, this work clarifies that even after a complete spinal transection, neurons in the cortex
483 still organize to convey information about the perturbation. it is important to note that, while our

484 microelectrode arrays were chronically implanted in the HLSMC, we do not assume that the same
485 neurons are being recorded pre-and post-SCI. Therefore, our conclusions are limited to the
486 average responses of neurons in the HLSMC at these two time points.

487 This responsiveness in the absence of ascending sensory feedback from the hindlimbs likely
488 originates from sensory signals from forelimb and trunk afferents caudal to the injury as well as
489 inputs from the visual and vestibular system. It has been shown that limb somatosensory afferents
490 are processed and even converge subcortically in the spinal cord and brainstem prior to reaching
491 the cortex (Allen et al. 1974; Azzena et al. 1983; Landgren and Silfvenius 1971; Sakamoto et al.
492 1987). Activity from the forelimbs is likely transmitted to the deafferented hindlimb cortex
493 producing sufficient activation to discriminate the severity of the tilt, with the delay reflecting the
494 additional time needed to reach firing thresholds due to the loss of hindlimb afferent inputs. While
495 the majority of hindlimb sensorimotor cortex cells respond to stimulation of the contralateral
496 hindlimb, forelimb afferents also send inputs to the hindlimb sensorimotor cortex. Therefore,
497 neurons in the "hindlimb" representation have been shown to respond to forelimb stimulation and
498 vice versa (Moxon et al. 2008). Additionally, a network of HLSMC neurons that are normally active
499 in response to forelimb movements could be contributing to the responses we observed in the
500 deafferented cortex. This would be in line with the work by Karayannidou et al, in which a subset
501 of cortical neurons followed the forelimbs more closely when the forelimbs and hindlimbs were
502 tilted out of phase (Karayannidou et al. 2008).

503 **Neural Encoding of Tilt**

504 Neurons have been shown to encode for multiple sensory and motor events by scaling their firing
505 rate to a parameter of the movement. For example, using multiple linear regressions, cells in the
506 motor cortex have been shown to modulate their firing rate depending on the speed, direction,
507 position and acceleration of arm trajectory (Ashe and Georgopoulos 1994). Moreover, neurons in

the motor cortex have been shown to increase their firing rate with finger velocity in a center-out task (Moran and Schwartz 1999). In sensory systems, cortical firing rate has been shown to increase with speed of whisker deflection (Pinto et al. 2013). Our findings extend this scaling of neuronal activity to the hindlimb cortex during postural events and show that the magnitude of the response is scaled to the severity of the tilt, encoding not only that a tilt occurred, but the severity of the tilt.

Therefore, not surprisingly, the information that a tilt occurred increased as the severity of the tilt increased. We show that this is certainly due to the increase in neuronal response magnitude as intensity of tilt increases (e.g. scaling), since holding the number of responsive neurons constant resulted in more information for greater intensity tilts. Of course, the central nervous system (CNS) has access to the information from additional neurons that respond, and it is likely that this information is used by the CNS to make appropriate postural adjustments in response to the tilt. A likely explanation for the greater number of neurons responding as the intensity of the tilt increases is the need to activate more motor neurons, in turn activating more muscle groups, to maintain balance in response to larger perturbations.

Spinal cord injury reduces the amount of information about tilt detection and tilt discrimination, even when neuron numbers were held constant. This reduction in information suggests that recruiting more neurons into the task is one strategy to ameliorate any loss of information after SCI. After complete mid-thoracic spinal cord transection, neurons in the HLSMC are more likely to both respond to forelimb stimulation and also activate trunk musculature after regular physical rehabilitation (Manohar et al. 2017). This cortical plasticity has been shown to improve behavioral outcome, as lesioning this reorganized cortex reduced gains in weight-supported stepping achieved by animals that received therapy (Manohar et al. 2017). Therefore, therapeutic interventions that support reorganization would be expected to further improve outcome, and therapy along the entire neural axis – including the cortex – is likely necessary to optimize

outcome after SCI (Ganzer et al. 2018; Krucoff et al. 2016; Sayenko et al. 2018; Taccola et al. 2018, 2020).

Finally, the sustained encoding of postural information after SCI observed in thus study (with respect to both stimulus detection as well as discrimination) has important translational implications for the field of neuroengineering. Despite playing a less significant role in postural control than other supraspinal centers in the brainstem, this study has demonstrated that the cortex can serve as a source of information about postural perturbations after SCI. Brain-machine interfaces can be developed using cortical signals to augment postural control, such as through spinal or peripheral nerve stimulation to support functional recovery after spinal cord injury.

Figure Legends

Figure 1: Experimental design

(a) Location of one of two bilaterally-implanted cortical arrays over hindlimb sensorimotor cortex overlapping with trunk motor cortex (adapted from (Leergaard et al. 2004)). (b) Diagram of the tilt task. At baseline, the animal stands on a platform with left hindlimb, right hindlimb, and forelimb force sensors. The platform makes unpredictable tilts of varying speed and direction in the horizontal plane described in (c). Neuron spiking activity is recorded throughout task, and an exemplar neuron's raster plot and PSTH for a specific tilt is shown. (c) Platform angle (top) and velocity (bottom) profiles for the 8 different tilt types in one direction: 4 "constant duration tilts" with varying final angle and peak velocity (i), 2 "constant final angle tilts" with varying duration and peak velocity (ii), and 2 "constant peak velocity tilts" of varying duration and final angle (iii). Note that each tilt includes the increase to max speed and then comes to a complete stop to include the effects of acceleration and deceleration. (d) Description of the PSTH-based method for classifying trials adapted from. (d) Description of the PSTH-based method for classifying trials (Adapted from Bridges et al. 2018). PSTH templates are generated for every neuron from over at least 100 of each tilt or baseline epoch. The PSTH from an individual trial is then compared to each template bin by bin, and the single trial is classified as belonging to the template with the most similarity (in this case, Tilt Type #2). A confusion matrix is generated from the classifier performance and information is calculated using Shannon's equation.

Figure 2: Ground reaction forces during tilts

Negative forces imply unloading whereas positive forces imply loading. (a) Average force measured in the left hindlimb (left) and both forelimbs (right) by the sensor for fast (270ms) and

slow (620ms) constant-angle tilts from tilt onset to the maximum tilt angle in the counterclockwise direction over 100 trials for a single animal. Forces are normalized such that each trial begins with 0 N of force. Shaded areas represent the standard error of the mean. Dotted vertical lines represent the time at which the platform reaches the maximum tilt angle for fast (270ms) and slow (620ms) tilts. Inset shows the same animal's forces for tilts in the clockwise direction. (b) The average maximum force applied to the left hindlimb force detector between approximately 100-200ms during counterclockwise tilts. (c) The timing of maximum force applied to the hindlimb force detector in (b). (d) The magnitude of the force applied to the hindlimb force detector during tilt at the end of the tilt (when the tilt platform achieves its maximum angle). (e) Forelimb forces were also evaluated. The maximum loading force applied to the forelimb force detector was calculated and compared across tilt types and Tx status. Note: only one sensor was used for forelimb force measurements, and animals' weight was partially supported by a trunk harness PostTx. Means and standard deviations are plotted over 99 individual trial data points both Pre- and PostTx. ****$p < 0.001$, ***$p < 0.001$, **$p < 0.01$, *$p<0.05$ (Bonferroni corrected).

Figure 3: Neuron response profiles for all tilt types Pre- and PostTx

For tilts of different duration, final angle, and peak velocity profiles (see inset table), the number of neurons and their average response metrics were calculated and compared. If a neuron responded to more than one tilt type, it was only included in the tilt type that led to its largest response. (a) Average number of neurons per animal responsive to each tilt type Pre- (n=10) and PostTx (n=8). (b) Average neuron firing rate (in Hz) throughout response. (c) Average duration of neuronal response. (d) Average latency of response onset, defined as the time at which the first bin surpasses threshold. (Inset) Table defining the tilt types for (a-d). Means and standard deviations are plotted over individual data points representing animals in (a) or individual neurons in (b-d). Total neuron numbers for each tilt type (in b-d): A1 (PreTx: 120; PostTx: 36), A2 (PreTx: 116; PostTx: 63), A3 (PreTx:132; PostTx: 71), A4 (PreTx: 152; PostTx: 90), B1 (PreTx: 147; PostTx: 69), B2 (PreTx: 155; PostTx: 90), C1 (PreTx: 115; PostTx: 37), C2 (PreTx: 117; PostTx: 30). ****$p < 0.001$, ***$p < 0.001$, **$p < 0.01$, *$p<0.05$ (Bonferroni corrected).

Figure 4. Neuron response classification

For the four tilts of constant duration but increasing peak velocity and tilt angle, neurons were categorized as being selective, nonselective, or scaled. (a-c) Exemplar peri-stimulus time histograms of neurons for each classification type, where (a) represents a neuron responsive to only one tilt type, (b) represents a neuron responsive to 2-3 tilt types, and (c) represents a scaled neuron, or a neuron responsive to all four tilt types. (d) Distribution of each neuron type before and after Tx. (e) Distribution of preferred event for all selective neurons before and after Tx. ***$p < 0.001$, **$p < 0.01$.

Figure 5. Relating average neural firing rate to hindlimb ground reaction forces throughout tilts

Trial-averaged left hindlimb ground reaction forces and neural firing rates (calculated as average spikes across all responsive neurons per 10ms bin) are plotted for tilts in the

counterclockwise (left plots) and clockwise (right plots) directions from the time of tilt onset (black dot) to the time of maximum tilt angle (red dot) for a single animal. A second animal's results are inset for comparison. Force and neural firing rate were zeroed at the start of tilt. (a) Comparison between fast and slow velocity tilts in the PreTx condition in the counterclockwise (left) and clockwise (right) directions. (b) Comparison between fast tilts in the Pre- and PostTx condition for the same animals in the clockwise (left) and counterclockwise (right) directions.

Figure 6. Information in the hindlimb cortex about tilts.

Information about (a) tilt detection and (b) tilt discrimination was calculated using the PSTH classifier (see Methods) for the four constant duration tilts of increasing peak velocity and final angle. (a) Tilt detection, or the ability to distinguish stance from the tilt, increased as a function of tilt severity ($p<0.0001$) in both the Pre- and PostTx condition, even with a significant decrease in information PostTx ($p<0.0001$). This was despite standardizing the number of neurons in all tilt and Tx states. Means and standard deviations plotted over individual data points. (b-c) Tilt discrimination, or the ability to differentiate one tilt type from the other three, increased with (b) adding more neurons ($p<0.0001$) as well as with (c) using a set number of neurons but increasing the length of recording supplied to the classifier ($p<0.0001$). Both instances demonstrated a reduction in information PostTx ($p<0.0001$ & $p<0.0001$), respectively. For both (b) and (c), solid line represents the change in mean for each condition, plotted over data points for individual animals (PreTx n= 10; PostTx n = 8).

References

Adkins DAL, **Boychuk J**, **Remple MS**, **Kleim JA**. Motor training induces experience-specific patterns of plasticity across motor cortex and spinal cord. *J. Appl. Physiol.* 2006.

Allen GI, **Azzena GB**, **Ohno T**. Somatotopically organized inputs from fore- and hindlimb areas of sensorimotor cortex to cerebellar Purkyně cells. *Exp Brain Res* , 1974. doi:10.1007/BF00238316.

Antri M, **Orsal D**, **Barthe JY**. Locomotor recovery in the chronic spinal rat: Effects of long-term treatment with a 5-HT2 agonist. *Eur J Neurosci* 16: 467–476, 2002.

Ashe J, **Georgopoulos AP**. Movement parameters and neural activity in motor cortex and area 5. *Cereb cortex* 4: 590–600, 1994.

Azzena GB, **Mameli O**, **Tolu E**. Convergence of central and peripheral signals on vestibular cells. *Acta Otolaryngol* , 1983. doi:10.3109/00016488309130942.

Barbeau H, **Ladouceur M**, **Mirbagheri MM**, **Kearney RE**. The effect of locomotor training combined with functional electrical stimulation in chronic spinal cord injured subjects: Walking and reflex studies. *Brain Res. Rev.* 2002.

Barbeau H, **Rossignol S**. The effects of serotonergic drugs on the locomotor pattern and on cutaneous reflexes of the adult chronic spinal cat. *Brain Res* , 1990. doi:10.1016/0006-8993(90)90435-E.

Beloozerova IN, **Sirota MG**, **Orlovsky GN**, **Deliagina TG**. Activity of pyramidal tract neurons in the cat during postural corrections. *J Neurophysiol* 93: 1831–1844, 2005.

Beloozerova IN, **Sirota MG**, **Swadlow HA**, **Orlovsky GN**, **Popova LB**, **Deliagina TG**. Activity of different classes of neurons of the motor cortex during postural corrections. *J Neurosci* 23: 7844–7853, 2003.

Beloozerova IN, **Zelenin P V.**, **Popova LB**, **Orlovsky GN**, **Grillner S**, **Deliagina TG**. Postural control in the rabbit maintaining balance on the tilting platform. *J Neurophysiol* 90: 3783–3793, 2006.

Van Den Brand R, **Heutschi J**, **Barraud Q**, **DiGiovanna J**, **Bartholdi K**, **Huerlimann M**, **Friedli L**, **Vollenweider I**, **Moraud EM**, **Duis S**, **Dominici N**, **Micera S**, **Musienko P**, **Courtine G**. Restoring voluntary control of locomotion after paralyzing spinal cord injury. *Science (80-)* 336: 1182–1185, 2012.

Bridges NR, **Meyers M**, **Garcia J**, **Shewokis PA**, **Moxon KA**. A rodent brain-machine interface paradigm to study the impact of paraplegia on BMI performance. *J Neurosci Methods* 306: 103–114, 2018.

Brustein E, **Rossignol S**. Recovery of locomotion after ventral and ventrolateral spinal lesions in the cat. I. Deficits and adaptive mechanisms. *J Neurophysiol* , 1998. doi:10.1152/jn.1998.80.3.1245.

Brustein E, **Rossignol S**. Recovery of locomotion after ventral and ventrolateral spinal lesions in the cat. II. Effects of noradrenergic and serotoninergic drugs. *J Neurophysiol* , 1999. doi:10.1152/jn.1999.81.4.1513.

Chvatal SA, **Macpherson JM**, **Torres-Oviedo G**, **Ting LH**. Absence of postural muscle synergies for balance after spinal cord transection. *J Neurophysiol* 110: 1301–1310, 2013.

Deliagina TG, **Sirota MG**, **Zelenin P V.**, **Orlovsky GN**, **Beloozerova IN**. Interlimb postural coordination in the standing cat. *J Physiol* 573: 211–224, 2006.

Dietz V, **Horstmann GA**, **Berger W**. Interlimb coordination of leg-muscle activation during perturbation of stance in humans. *J Neurophysiol* , 1989. doi:10.1152/jn.1989.62.3.680.

Dietz V, **Quintern J**, **Berger W**, **Schenck E**. Cerebral potentials and leg muscle e.m.g. responses associated with stance perturbation. *Exp Brain Res* , 1985. doi:10.1007/BF00236540.

Edgerton VR, **Leon RD**, **Harkema SJ**, **Hodgson JA**, **London N**, **Reinkensmeyer DJ**, **Roy RR**, **Talmadge RJ**, **Tillakaratne NJ**, **Timoszyk W**, **Tobin A**. Retraining the injured spinal cord. *J. Physiol.* 2001.

Edgerton VR, **Tillakaratne NJK**, **Bigbee AJ**, **De Leon RD**, **Roy RR**. Plasticity of the spinal neural circuitry after injury. *Annu. Rev. Neurosci.* 2004.

Foffani G, **Moxon KA**. PSTH-based classification of sensory stimuli using ensembles of single neurons. *J Neurosci Methods* 135: 107–120, 2004.

Fujio K, **Obata H**, **Kitamura T**, **Kawashima N**, **Nakazawa K**. Corticospinal excitability is modulated as a function of postural perturbation predictability. *Front Hum Neurosci* , 2018. doi:10.3389/fnhum.2018.00068.

Fung J, **Macpherson JM**. Attributes of quiet stance in the chronic spinal cat. *J Neurophysiol* 82: 3056–3065, 1999.

Ganzer PD, **Darrow MJ**, **Meyers EC**, **Solorzano BR**, **Ruiz AD**, **Robertson NM**, **Adcock KS**, **James JT**, **Jeong HS**, **Becker AM**, **Goldberg MP**, **Pruitt DT**, **Hays SA**, **Kilgard MP**, **Rennaker RL**. Closed-loop neuromodulation restores network connectivity and motor control after spinal cord injury. *Elife* , 2018. doi:10.7554/eLife.32058.

Ganzer PD, **Manohar A**, **Shumsky JS**, **Moxon KA**. Therapy induces widespread reorganization of motor cortex after complete spinal transection that supports motor recovery. *Exp Neurol* 279: 1–12, 2016.

Ganzer PD, **Moxon KA**, **Knudsen EB**, **Shumsky JS**. Serotonergic pharmacotherapy promotes cortical reorganization after spinal cord injury. *Exp Neurol* 241: 84–94, 2013.

Ghosh A, **Sydekum E**, **Haiss F**, **Peduzzi S**, **Zörner B**, **Schneider R**, **Baltes C**, **Rudin M**, **Weber B**, **Schwab ME**. Functional and anatomical reorganization of the sensory-motor cortex after incomplete spinal cord injury in adult rats. *J Neurosci* 29: 12210–9, 2009.

Giuliani CA, **Smith JL**. Development and characteristics of airstepping in chronic spinal cats. *J Neurosci* , 1985. doi:10.1523/jneurosci.05-05-01276.1985.

Harkema S, **Gerasimenko Y**, **Hodes J**, **Burdick J**, **Angeli C**, **Chen Y**, **Ferreira C**, **Willhite A**, **Rejc E**, **Grossman RG**, **Reggie Edgerton V**. Effect of epidural stimulation of the lumbosacral spinal cord on voluntary movement, standing, and assisted stepping after motor complete paraplegia: A case study. *Lancet* 377: 1938–1947, 2011.

Honeycutt CF, **Nichols TR**. The decerebrate cat generates the essential features of the force constraint strategy. *J Neurophysiol* , 2010. doi:10.1152/jn.00764.2009.

Horak FB, **Macpherson JM**. Postural Orientation and Equilibrium. In: *Comprehensive Physiology*. 1996.

Ichiyama RM, **Gerasimenko YP**, **Zhong H**, **Roy RR**, **Edgerton VR**. Hindlimb stepping movements in complete spinal rats induced by epidural spinal cord stimulation. *Neurosci Lett* 383: 339–344, 2005.

Jacobs J V, **Fujiwara K**, **Tomita H**, **Furune N**, **Kunita K**, **Horak FB**. Changes in the activity of the cerebral cortex relate to postural response modification when warned of a perturbation. *Clin Neurophysiol* 119: 1431–42, 2008.

Jiang W, **Drew T**. Effects of bilateral lesions of the dorsolateral funiculi and dorsal columns at the level of the low thoracic spinal cord on the control of locomotion in the adult cat. I. Treadmill walking. *J Neurophysiol* , 1996. doi:10.1152/jn.1996.76.2.849.

Kao T, **Shumsky JS**, **Knudsen EB**, **Murray M**, **Moxon KA**. Functional role of exercise-induced cortical organization of sensorimotor cortex after spinal transection. *J Neurophysiol* 106: 2662–

74, 2011.

Karayannidou A, **Deliagina TG**, **Tamarova ZA**, **Sirota MG**, **Zelenin P V.**, **Orlovsky GN**, **Beloozerova IN**. Influences of sensory input from the limbs on feline corticospinal neurons during postural responses. *J Physiol* 586: 247–263, 2008.

Kellog WN, **Deese J**, **Pronko NH**. On the behavior of the lumbo-spinal dog. *J Exp Psychol* , 1946. doi:10.1037/h0060016.

Kilkenny C, **Browne W**, **Cuthill IC**, **Emerson M**, **Altman DG**. Animal research: Reporting in vivo experiments: The ARRIVE guidelines. *Br. J. Pharmacol.* 2010.

Knudsen EB, **Flint RD**, **Moxon K a**. Encoding of temporal intervals in the rat hindlimb sensorimotor cortex. *Front Syst Neurosci* 6: 67, 2012.

Krucoff MO, **Rahimpour S**, **Slutzky MW**, **Edgerton VR**, **Turner DA**. Enhancing Nervous System Recovery through Neurobiologics, Neural Interface Training, and Neurorehabilitation. *Front Neurosci* 10: 584, 2016.

Landgren S, **Silfvenius H**. Nucleus Z, the medullary relay in the projection path to the cerebral cortex of group I muscle afferents from the cat's hind limb. *J Physiol* , 1971. doi:10.1113/jphysiol.1971.sp009633.

Lavrov I, **Courtine G**, **Dy CJ**, **Van Den Brand R**, **Fong AJ**, **Gerasimenko Y**, **Zhong H**, **Roy RR**, **Edgerton VR**. Facilitation of stepping with epidural stimulation in spinal rats: Role of sensory input. *J Neurosci* 28: 7774–7780, 2008.

Lavrov I, **Gerasimenko YP**, **Ichiyama RM**, **Courtine G**, **Zhong H**, **Roy R**, **Edgerton VR**. Plasticity of spinal cord reflexes after a complete transection in adult rats: relationship to stepping ability. *J Neurophysiol* 96: 1699–710, 2006.

Leergaard TB, **Alloway KD**, **Pham TAT**, **Bolstad I**, **Hoffer ZS**, **Pettersen C**, **Bjaalie JG**. Three-dimensional topography of corticopontine projections from rat sensorimotor cortex: Comparisons with corticostriatal projections reveal diverse integrative organization. *J Comp Neurol* 478: 306–322, 2004.

De Leon RD, **Tamaki H**, **Hodgson JA**, **Roy RR**, **Edgerton VR**. Hindlimb locomotor and postural training modulates glycinergic inhibition in the spinal cord of the adult spinal cat. *J Neurophysiol* , 1999. doi:10.1152/jn.1999.82.1.359.

Lyalka VF, **Hsu LJ**, **Karayannidou A**, **Zelenin P V.**, **Orlovsky GN**, **Deliagina TG**. Facilitation of postural limb reflexes in spinal rabbits by serotonergic agonist administration, epidural electrical stimulation, and postural training. *J Neurophysiol* , 2011. doi:10.1152/jn.00115.2011.

Lyalka VF, **Orlovsky GN**, **Deliagina TG**. Impairment of postural control in rabbits with extensive spinal lesions. *J Neurophysiol* , 2009. doi:10.1152/jn.00009.2008.

Lyalka VF, **Zelenin P V**, **Karayannidou A**, **Orlovsky GN**, **Grillner S**, **Deliagina TG**. Impairment and recovery of postural control in rabbits with spinal cord lesions. *J Neurophysiol* 94: 3677–90, 2005.

Macpherson JM, **Fung J**. Weight support and balance during perturbed stance in the chronic spinal cat. *J Neurophysiol* 82: 3066–3081, 1999.

Macpherson JM, **Fung J**, **Jacobs R**. Postural orientation, equilibrium, and the spinal cord. *Adv. Neurol.* 1997.

Manohar A, **Flint RD**, **Knudsen E**, **Moxon KA**. Decoding hindlimb movement for a brain machine interface after a complete spinal transection. *PLoS One* 7: e52173, 2012.

Manohar A, **Foffani G**, **Ganzer PD**, **Bethea JR**, **Moxon KA**. Cortex-dependent recovery of unassisted hindlimb locomotion after complete spinal cord injury in adult rats. *Elife* 6: e23532, 2017.

Massion J, **Dufosse M**. Coordination Between Posture and Movement: Why and How? *Physiology* , 1988. doi:10.1152/physiologyonline.1988.3.3.88.

Moran DW, **Schwartz AB**. Motor Cortical Representation of Speed and Direction During Reaching Motor Cortical Representation of Speed and Direction During Reaching. *J Neurophysiol* 82: 2676–2692, 1999.

Moxon KA, **Hale LL**, **Aguilar J**, **Foffani G**. Responses of infragranular neurons in the rat primary somatosensory cortex to forepaw and hindpaw tactile stimuli. *Neuroscience* 156: 1083–92, 2008.

Musienko PE, **Zelenin P V.**, **Lyalka VF**, **Orlovsky GN**, **Deliagina TG**. Postural performance in decerebrated rabbit. *Behav Brain Res* , 2008. doi:10.1016/j.bbr.2008.02.011.

Musienko PE, **Zelenin P V.**, **Orlovsky GN**, **Deliagina TG**. Facilitation of postural limb reflexes with epidural stimulation in spinal rabbits. *J Neurophysiol* , 2010. doi:10.1152/jn.00575.2009.

Nandakumar B, **Blumenthal GH**, **Pauzin FP**, **Moxon KA**. Trunk sensory and motor cortex is preferentially integrated with hindlimb sensory information that supports trunk stabilization. *bioRxiv* , 2020.

Orlovsky GN, **Deliagina TG**, **Grillner S**. Neuronal Control of Locomotion: From Mollusc to Man (Oxford Neuroscience S): 9780198524052: Medicine & Health Science Books @ Amazon.com. *Oxford Univ. Press* 1999.

Pinto DJ, **Brumberg JC**, **Simons DJ**. Circuit Dynamics and Coding Strategies in Rodent Somatosensory Cortex Circuit Dynamics and Coding Strategies in Rodent Somatosensory Cortex. 1158–1166, 2013.

Pratt CA, **Fung J**, **Macpherson JM**. Stance control in the chronic spinal cat. *J Neurophysiol* , 1994. doi:10.1152/jn.1994.71.5.1981.

Rath M, **Vette AH**, **Ramasubramaniam S**, **Li K**, **Burdick J**, **Edgerton VR**, **Gerasimenko YP**, **Sayenko DG**. Trunk Stability Enabled by Noninvasive Spinal Electrical Stimulation after Spinal Cord Injury. *J Neurotrauma* , 2018. doi:10.1089/neu.2017.5584.

Rossignol S, **Bouyer L**, **Barthélemy D**, **Langlet C**, **Leblond H**. Recovery of locomotion in the cat following spinal cord lesions. *Brain Res. Rev.* 2002.

Rossignol S, **Drew T**, **Brustein E**, **Jiang W**. Locomotor performance and adaptation after partial or complete spinal cord lesions in the cat. *Prog Brain Res* , 1999. doi:10.1016/s0079-6123(08)62870-8.

Sakamoto T, **Porter LL**, **Asanuma H**. Long-lasting potentiation of synaptic potentials in the motor cortex produced by stimulation of the sensory cortex in the cat: A basis of motor learning. *Brain Res* 413: 360–364, 1987.

Sayenko DG, **Atkinson DA**, **Mink AM**, **Gurley KM**, **Edgerton VR**, **Harkema SJ**, **Gerasimenko YP**. Vestibulospinal and Corticospinal Modulation of Lumbosacral Network Excitability in Human Subjects. *Front Physiol* , 2018. doi:10.3389/fphys.2018.01746.

Shah PK, **Sureddi S**, **Alam M**, **Zhong H**, **Roy RR**, **Edgerton VR**, **Gerasimenko Y**. Unique spatiotemporal neuromodulation of the lumbosacral circuitry shapes locomotor success after spinal cord injury. *J Neurotrauma* 33: 1709–1723, 2016.

Sławińska U, **Majczyński H**, **Dai Y**, **Jordan LM**. The upright posture improves plantar stepping and alters responses to serotonergic drugs in spinal rats. *J Physiol* , 2012. doi:10.1113/jphysiol.2011.224931.

Taccola G, **Gad P**, **Culaclii S**, **Wang PM**, **Liu W**, **Edgerton VR**. Acute neuromodulation restores spinally-induced motor responses after severe spinal cord injury. *Exp Neurol* , 2020. doi:10.1016/j.expneurol.2020.113246.

Taccola G, **Sayenko D**, **Gad P**, **Gerasimenko Y**, **Edgerton VR**. And yet it moves: Recovery of volitional control after spinal cord injury. *Prog. Neurobiol.* 2018.

Figure 1

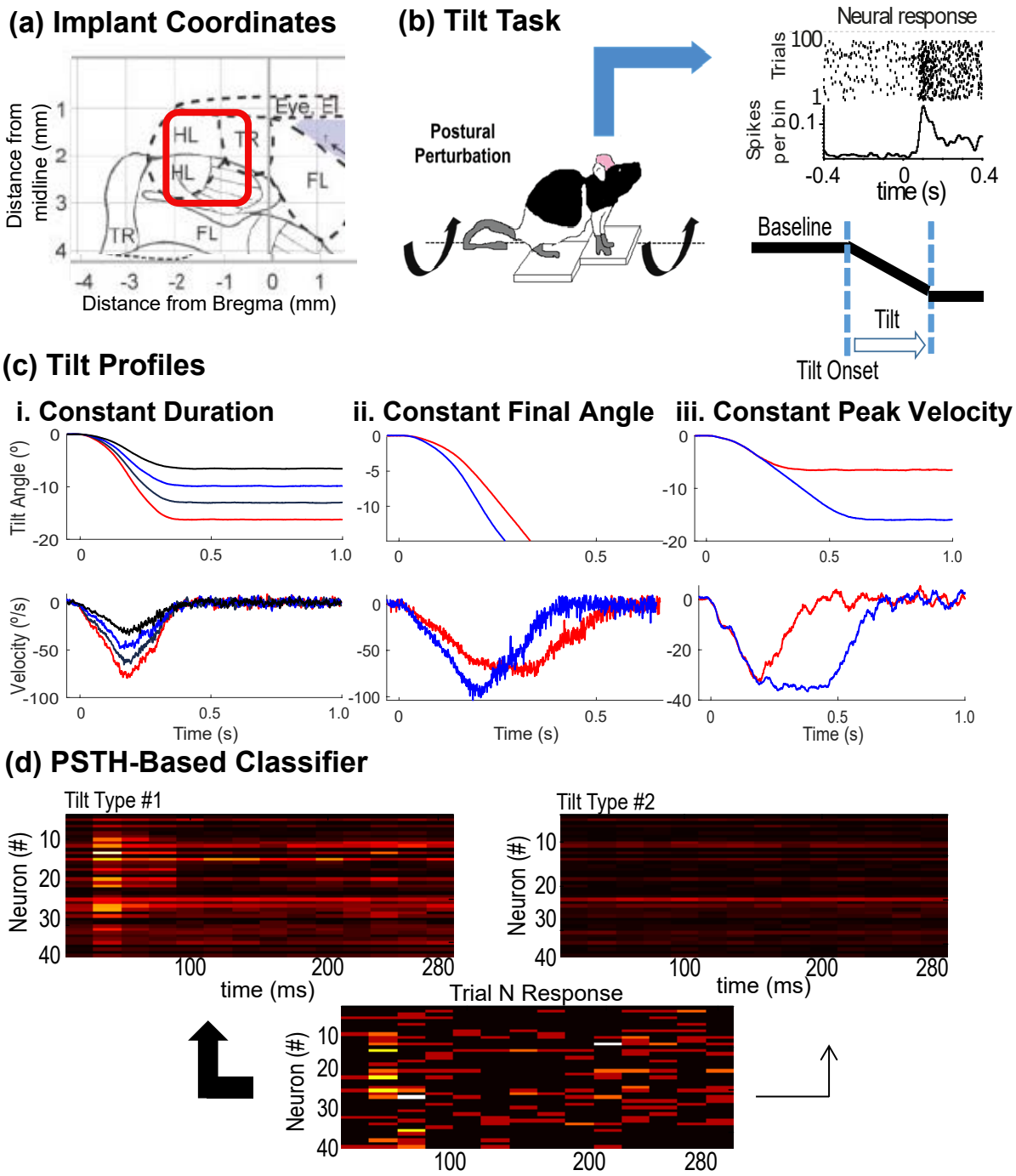
(a) Implant Coordinates
Distance from midline (mm)
Distance from Bregma (mm)
HL
TR
FL
Eye
(b) Tilt Task
Postural Perturbation
Neural response
Trials
Spikes per bin
time (s)
Baseline
Tilt
Tilt Onset
(c) Tilt Profiles
i. Constant Duration
ii. Constant Final Angle
iii. Constant Peak Velocity
Tilt Angle (°)
Velocity (°/s)
Time (s)
(d) PSTH-Based Classifier
Tilt Type #1
Tilt Type #2
Neuron (#)
time (ms)
Trial N Response

Figure 2

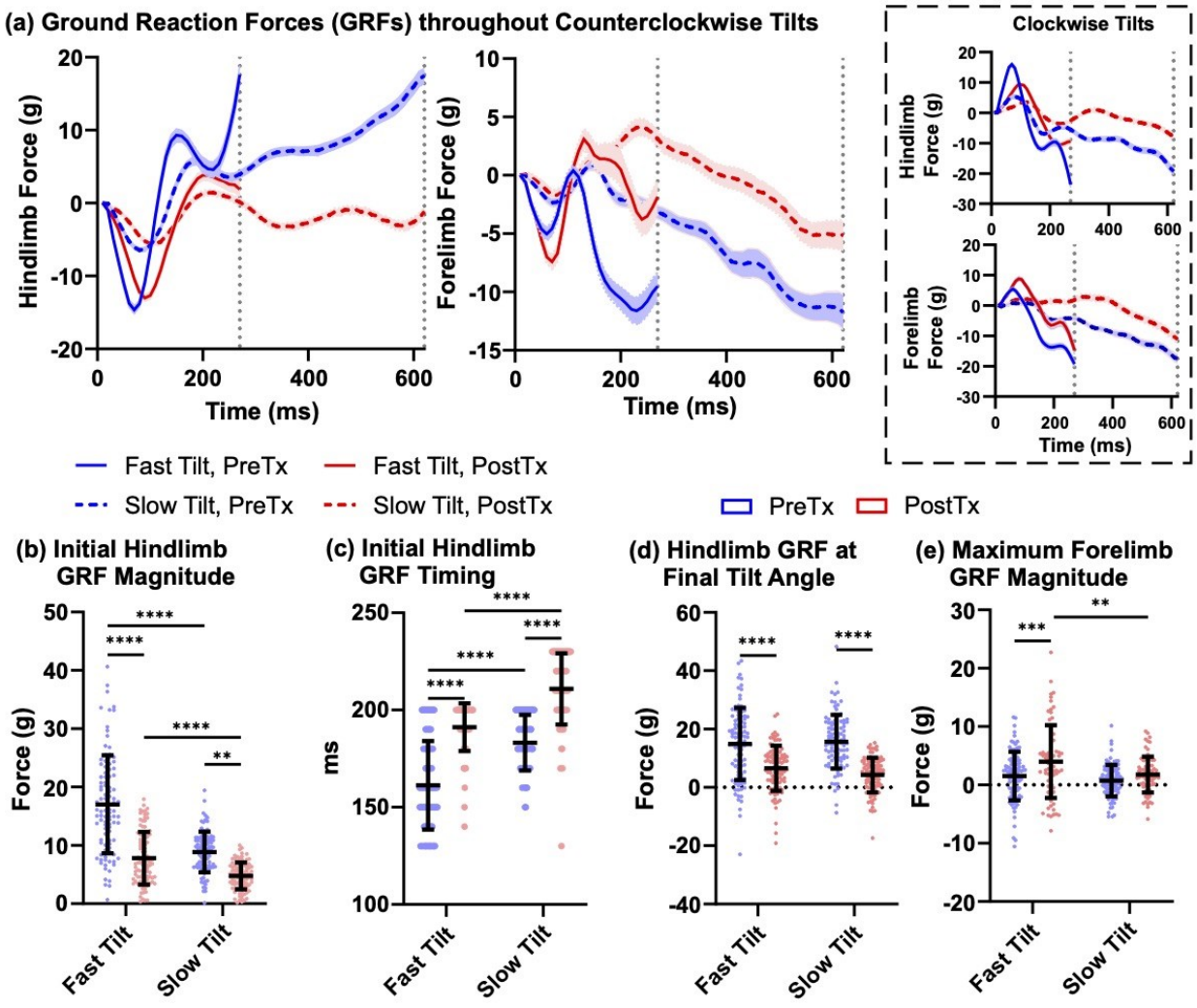
(a) Ground Reaction Forces (GRFs) throughout Counterclockwise Tilts
Hindlimb Force (g)
Forelimb Force (g)
Time (ms)
Clockwise Tilts
Fast Tilt, PreTx
Fast Tilt, PostTx
Slow Tilt, PreTx
Slow Tilt, PostTx
PreTx
PostTx
(b) Initial Hindlimb GRF Magnitude
(c) Initial Hindlimb GRF Timing
(d) Hindlimb GRF at Final Tilt Angle
(e) Maximum Forelimb GRF Magnitude
Force (g)
ms
Fast Tilt
Slow Tilt

Figure 3

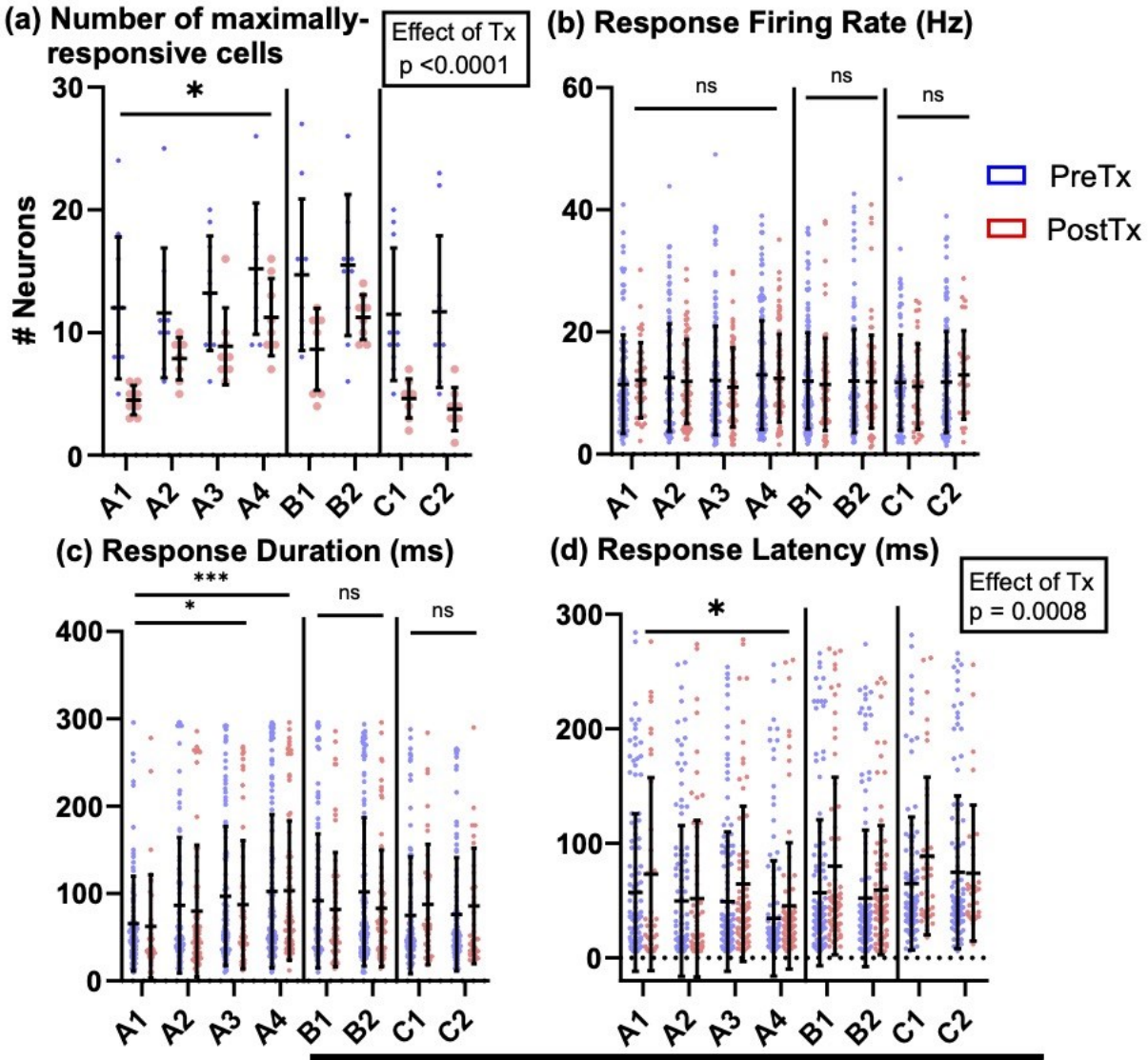

		Tilt							
		A1	A2	A3	A4	B1	B2	C1	C2
Parameter	Dur. (ms)	**280**	**280**	**280**	**280**	258	198	310	574
	Final Angle (◦)	6.6	9.7	13.5	16.6	**11.2**	**11.2**	6.6	16.3
	Peak Vel(◦/s)	32.4	47.4	63.0	77.7	68.9	91.5	**32.4**	**32.4**

Figure 4

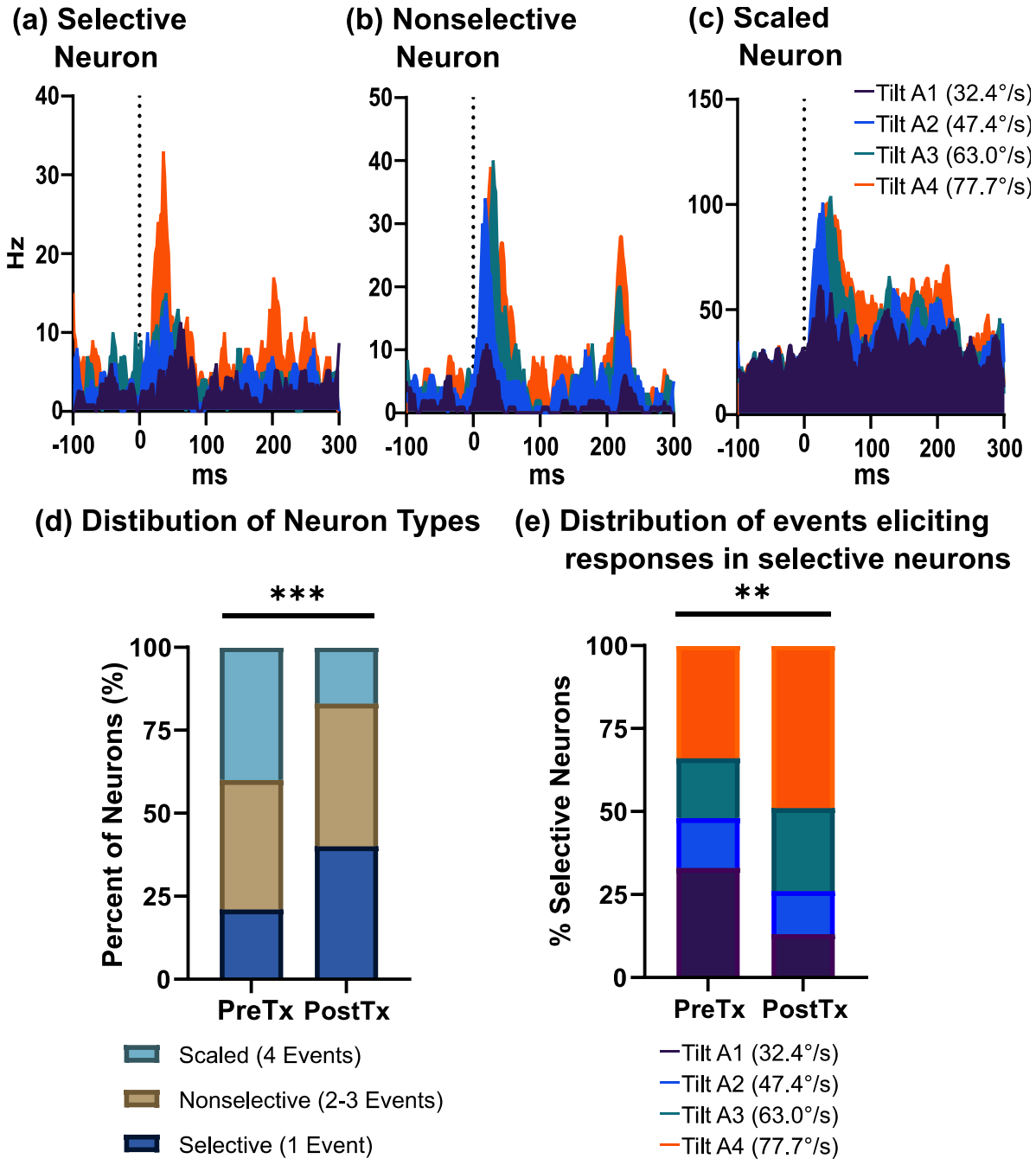
(a) Selective Neuron
(b) Nonselective Neuron
(c) Scaled Neuron
Hz
ms
Tilt A1 (32.4°/s)
Tilt A2 (47.4°/s)
Tilt A3 (63.0°/s)
Tilt A4 (77.7°/s)
(d) Distibution of Neuron Types
(e) Distribution of events eliciting responses in selective neurons
***
**
Percent of Neurons (%)
% Selective Neurons
PreTx
PostTx
Scaled (4 Events)
Nonselective (2-3 Events)
Selective (1 Event)

Figure 5

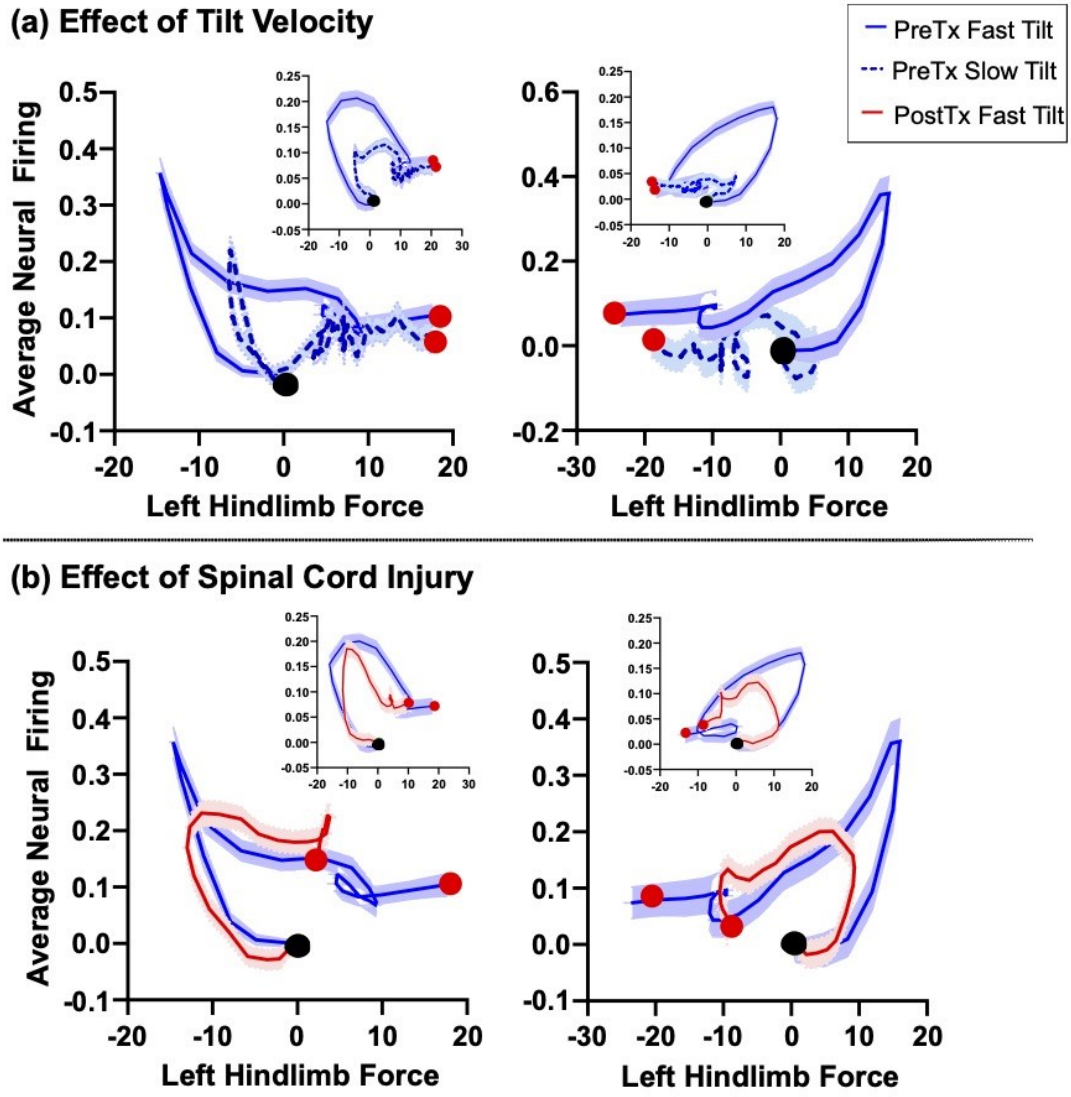
(a) Effect of Tilt Velocity
PreTx Fast Tilt
PreTx Slow Tilt
PostTx Fast Tilt
Average Neural Firing
Left Hindlimb Force
Left Hindlimb Force
(b) Effect of Spinal Cord Injury
Average Neural Firing
Left Hindlimb Force
Left Hindlimb Force

Figure 6

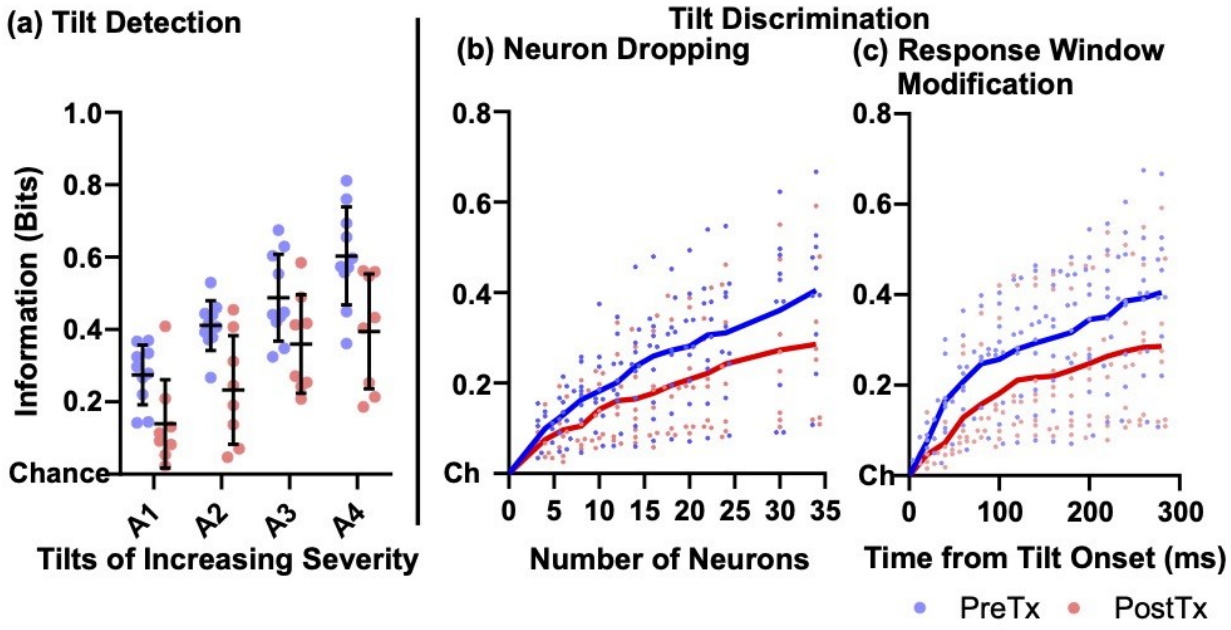
(a) Tilt Detection
Tilt Discrimination
(b) Neuron Dropping
(c) Response Window Modification
Information (Bits)
1.0
0.8
0.6
0.4
0.2
Chance
A1
A2
A3
A4
Tilts of Increasing Severity
0.8
0.6
0.4
0.2
Ch
0 5 10 15 20 25 30 35
Number of Neurons
0.8
0.6
0.4
0.2
Ch
0 100 200 300
Time from Tilt Onset (ms)
PreTx
PostTx